LETTERS

Oceanic nickel depletion and a methanogen famine before the Great Oxidation Event

Kurt O. Konhauser[1], Ernesto Pecoits[1], Stefan V. Lalonde[1], Dominic Papineau[2], Euan G. Nisbet[3], Mark E. Barley[4], Nicholas T. Arndt[5], Kevin Zahnle[6] & Balz S. Kamber[7]

It has been suggested that a decrease in atmospheric methane levels triggered the progressive rise of atmospheric oxygen, the so-called Great Oxidation Event, about 2.4 Gyr ago[1]. Oxidative weathering of terrestrial sulphides, increased oceanic sulphate, and the ecological success of sulphate-reducing microorganisms over methanogens has been proposed as a possible cause for the methane collapse[1], but this explanation is difficult to reconcile with the rock record[2,3]. Banded iron formations preserve a history of Precambrian oceanic elemental abundance and can provide insights into our understanding of early microbial life and its influence on the evolution of the Earth system[4,5]. Here we report a decline in the molar nickel to iron ratio recorded in banded iron formations about 2.7 Gyr ago, which we attribute to a reduced flux of nickel to the oceans, a consequence of cooling upper-mantle temperatures and decreased eruption of nickel-rich ultramafic rocks at the time. We measured nickel partition coefficients between simulated Precambrian sea water and diverse iron hydroxides, and subsequently determined that dissolved nickel concentrations may have reached ~400 nM throughout much of the Archaean eon, but dropped below ~200 nM by 2.5 Gyr ago and to modern day values[6] (~9 nM) by ~550 Myr ago. Nickel is a key metal cofactor in several enzymes of methanogens[7] and we propose that its decline would have stifled their activity in the ancient oceans and disrupted the supply of biogenic methane. A decline in biogenic methane production therefore could have occurred before increasing environmental oxygenation and not necessarily be related to it. The enzymatic reliance of methanogens on a diminishing supply of volcanic nickel links mantle evolution to the redox state of the atmosphere.

Did a nickel famine at the end of the Archaean cause catastrophic collapse of atmospheric methane and thereby facilitate the rise of atmospheric oxygen? At the heart of our hypothesis is the distinct topography in molar Ni/Fe ratios preserved in banded iron formations (BIF) over time (Fig. 1; see also Supplementary Figs 1–3, Supplementary Tables 1, 2). An expanded trace element database for BIF that includes more than 1,200 bulk and grain-by-grain (haematite, magnetite) measurements shows a trend in BIF Ni/Fe ratios that can be defined by two broad stages. Stage 1, which spans

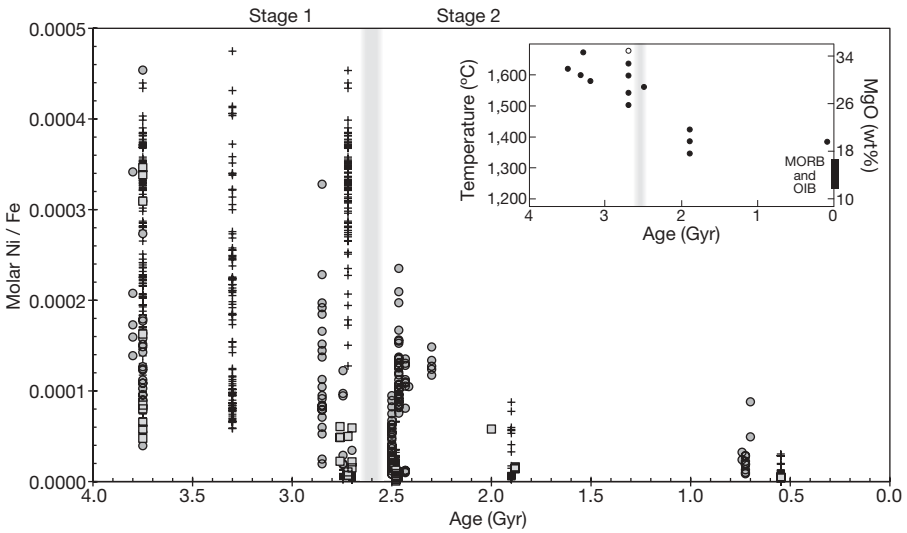

Figure 1 | Ni/Fe mole ratios for BIF versus age, and properties of parental komatiite liquids. The figure contains 1,214 measurements, including literature data (circles) and our new bulk (squares) and grain-by-grain laser ablation analyses (crosses). Two stages are identified based on maximal Ni/Fe ratios, with the transition period indicated by a grey bar. Inset, maximum MgO contents inferred for the parental komatiite liquids[19], and the probable eruption temperatures, plotted (filled circles) as a function of age. Eruption temperatures T were calculated using the relation $T = 1{,}000 + 20\mathrm{MgO}$ (where T is in °C, and MgO in wt%; ref. 18), assuming essentially anhydrous magmas. Open circle, recent data by Berry *et al.*[13]. MORB, mid-ocean-ridge basalts; OIB, oceanic island basalt.

[1]Department of Earth and Atmospheric Sciences, University of Alberta, Edmonton T6G 2E3, Canada. [2]Geophysical Laboratory, Carnegie Institution of Washington, 5251 Broad Branch Road NW, Washington DC 20015, USA. [3]Department of Earth Sciences, Royal Holloway University of London, Egham, Surrey TW20 0EX, UK. [4]School of Earth and Environment, University of Western Australia, 35 Stirling Highway, Crawley, Western Australia 6009, Australia. [5]Laboratoire de Géodynamique des Chaîne Alpines, Maison de Géosciences, Université Joseph Fourier, 1381 rue de la piscine, Grenoble 38041, France. [6]NASA Ames Research Center, MS 245-3, Moffett Field, California 94035, USA. [7]Department of Earth Sciences, Laurentian University, Sudbury, Ontario P3E 2C6, Canada.

from the oldest BIF (~3.8–3.7 Gyr) to those as young as 2.7 Gyr, shows a uniform maximum molar Ni/Fe ratio ($\sim 4.5 \times 10^{-4}$). Stage 2, which we demarcate at around 2.5 Gyr ago (the Archaean-Proterozoic boundary), shows strikingly lower maximal Ni/Fe ratios (below 2.2×10^{-4}). The boundary between stages 1 and 2, although at present not well constrained owing to gaps in the BIF record, marks a significant and irreversible decline in oceanic Ni concentrations: stage 1 values are never reached again. Stage 2 is characterized by a further steady decline in maximum Ni/Fe ratios, a trend that persists for the remainder of the Palaeoproterozoic BIF record. It is possible that a third stage exists, post-dating a resurgence in BIF deposition between 0.75 and 0.55 Gyr ago, but the scarcity of Neoproterozoic BIF trace element data precludes any further conclusion at present.

The transition from stage 1 to stage 2 is unlikely to have been driven by changes in Ni sinks, which appear to be relatively insensitive to evolving major element and redox conditions from Archaean-Palaeoproterozoic ferrous iron seas, through Mesoproterozoic sulphidic seas, to the onset of oxygenated bottom waters in the Neoproterozoic (ref. 8; their Fig. 4). Moreover, Fe^{2+} and Ni^{2+} show similar behaviour with increasing sulphide concentrations, indicating that the presence of sulphide will not lead to chemical fractionation between the two metals (ref. 8; their Fig. 2). In this regard, sulphide is not a major sink for Ni except for some magmatic sulphides (ref. 9, and references therein), and unlike Cu-Zn-Au, which are abundant in Precambrian volcanogenic massive sulphide deposits[10], there are no accumulations that would indicate sequestration of Ni into the sea floor of a sulphidic ocean[11]. The trends in our data also appear independent of oxidative mechanism or depositional environment. The prominent decline in molar Ni/Fe ratio is recorded in pre-Great Oxidation Event BIF (Supplementary Fig. 3) that appear to have been deposited in waters of greater than 200 m depth[12]. During stage 2, so-called granular iron formations of the circum-Ungava belt of North America (for example, the 1.88 Gyr Gunflint Formation) formed in shallow-water, high-energy environments[12], yet they show no discernable difference in Ni/Fe ratios from deep-water stage 2 BIF (for example, the 0.55 Gyr Yerbal Formation).

In contrast, Ni supply probably changed significantly with time. First, a hotter Archaean mantle[13] produced abundant Ni-rich komatiite and olivine-rich basalt in oceanic crust, plateaus, and perhaps on land[14,15]. Second, Archaean tholeiites, which made up most of the oceanic crust, were richer in Ni than their modern counterparts[16]. Third, a major peak in preserved komatiite abundance occurred during the most intense period of mantle plume magmatism and continental crustal growth in Earth's history, between 2.72 and 2.66 Gyr ago[14,17], after which their abundance decreased rapidly

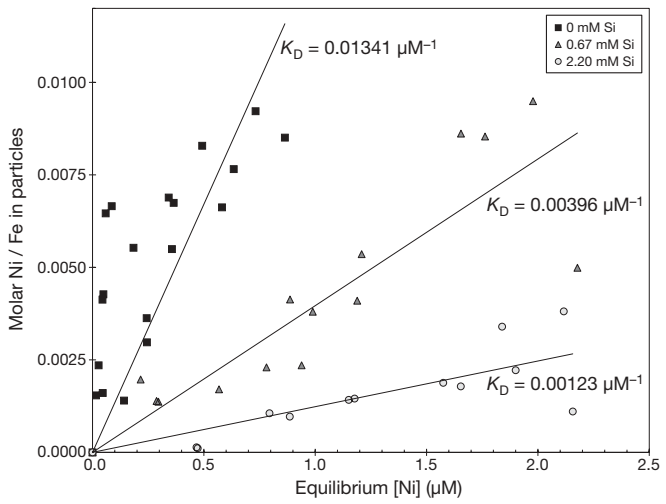

Figure 2 | Experimentally determined distribution coefficients for dissolved Ni. The K_d values were obtained during Ni co-precipitation with HFO, and in the presence of various concentrations of silica, as per ref. 5.

(see Supplementary Fig. 4, Supplementary Table 3). All of the above factors are related to the extent of mantle source melting and temperature[18], whose evolution can be reconstructed from the composition of mafic magmas (Fig. 1 inset)[19]. The hotter Archaean mantle produced more Ni-rich ultramafic rocks, resulting in a much greater supply of Ni than any time thereafter, a fact reflected in the similarity between the lava eruption temperature versus age curve and the molar Ni/Fe ratio of BIF. Nickel preserved in BIF was almost certainly supplied in dissolved form, as opposed to particulate material (that is, volcanic ash or clastic sediment). Supporting this are low concentrations of lithophile elements in BIF samples selected for this study (see Methods). Furthermore, the Cr/Ni ratios in Archaean BIF are lower than in Archaean basalts, komatiites and shales (Supplementary Fig. 5) which implies Ni mobilization during chemical weathering and hydrothermal alteration of Ni-bearing minerals and preferential supply of Ni (over Cr) to the ocean. Correspondingly, chemical analysis of Archaean basalt-derived palaeosols show accumulation of Cr and loss of Ni in their weathering profiles (see arrow, Supplementary Fig. 5).

The chemical archive preserved in BIF can be exploited using the predictable nature of adsorption reactions occurring at the surface of the authigenic hydrous ferric oxides (HFO) that would have originally precipitated from, and equilibrated with, contemporaneous seawater (see Supplementary Discussion). In natural systems, where trace element sequestration by HFO results from a continuum of adsorption and co-precipitation reactions, lumped-process distribution coefficient models can be used to relate the concentration of an element in the precipitate to the dissolved concentration present at the time of precipitation. In fact, this predictive aspect of HFO sorption reactions has been used to better understand the BIF record with respect to limitations on Precambrian primary productivity that may have arisen via HFO sequestration of bio-essential nutrients[4,5].

Nickel partition coefficients were determined for HFO precipitated in the presence of dissolved silica (Fig. 2). Assumptions made in our experiments and extrapolation include an ocean pH of 7–8, ionic strength ~0.5 M, seawater Si/Fe molar ratios of ~12/1 (as per ref. 5), and minimal remobilization of Ni during post-depositional diagenesis and/or metamorphism (see Supplementary Discussion). The experimentally determined partition coefficients allow a first-order estimation of the evolution of seawater Ni concentration from the solid-phase BIF data presented in this study. Figure 2 displays approximately linear relationships between dissolved Ni and the Ni/Fe ratio in the various HFOs examined, consistent with dissolved Ni concentrations well below those approaching site saturation for these particles. Different amounts of dissolved silica, which was added to the experiments to simulate waters at saturation with respect to cristobalite (0.67 mM) or amorphous silica (2.20 mM), had a pronounced effect on HFO reactivity (see Methods for the rationale of these silica concentrations). As Fe(III) hydrolyses and precipitates at circum-neutral pH, dissolved silica is incorporated into the particles, altering their surface properties, and also directly out-competing other dissolved ions for adsorption sites[5]. Using the Si-rich particles as the best proxy for particle composition in the Archaean, extrapolated dissolved Ni concentrations (Fig. 3) suggest that BIF record a drastic reduction in dissolved Ni, from values as high as ~400 nM to values no greater than 200 nM during the transition from stage 1 to stage 2; stage 2 shows a gradual decline to <50 nM by 0.7 Gyr ago, with modern ocean values reached some time after 0.55 Gyr ago. Although it is difficult to quantify the uncertainty in our extrapolation from HFO sorption experiments to the ancient oceans, we feel that this approach is the best currently available for estimating palaeo-ocean Ni concentration. Moreover, we have deliberately taken a conservative approach, as any Ni loss that might have occurred during post-depositional alteration of HFO would lead to an underestimate of oceanic Ni concentrations.

Our finding of nickel-rich Archaean oceans has immediate implications for microbial life that requires it as a trace element. It has been previously suggested that nickel-containing enzymes are remnants from

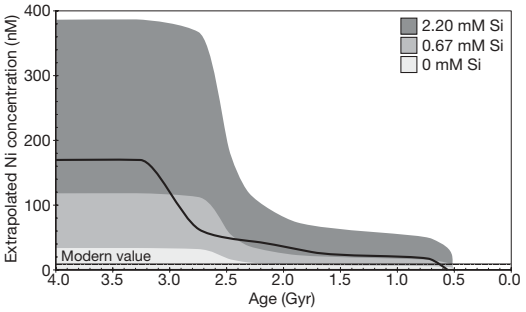

Figure 3 | Maximum dissolved Ni concentrations in sea water through time. Values were extrapolated from solid-phase BIF Ni/Fe data using experimentally determined Ni distribution coefficients. The three shaded areas represent maximum aqueous Ni concentrations at dissolved silica concentrations of 2.20 mM (dark grey), 0.67 mM (medium grey) and 0 mM (light grey). The solid black line represents the average dissolved Ni value from time-averaged Ni/Fe ratios as calculated in Supplementary Fig. 3. The modern mean oceanic Ni concentration (9 nM; ref. 6) is plotted as a line.

an early period in microbial evolution when nickel was abundant[20]. Specifically, methanogens require Ni for the synthesis of three different [NiFe]-hydrogenases, carbon monoxide dehydrogenase, acetyl-CoA synthase/decarbonylase, and methyl-coenzyme M reductase (MCR), the latter being the catalyst of the final methane-forming step[7]. These nickel enzymes are present in high concentrations, with MCR accounting for approximately 10% of methanogen cytoplasmic proteins. Crucially, although methanogens may continue to grow in the absence of Ni (although some have reported cell autolysis when Ni is absent)[21], the synthesis of co-factor F_{430}, the numbers of methanogen cells, and methane production all depend strongly on dissolved Ni availability. For example, co-factor F_{430} content on a per-cell basis increases with Ni concentrations over a 75–2,500 nM range[22], whereas methanogen cell numbers are strongly Ni-limited at concentrations below 100 nM (ref. 23). Similarly, it has been demonstrated[24] that methane production in continuous culture decreased progressively when Ni concentrations were reduced from 8,500 nM to 250 nM, the lowest concentration examined by these authors. Not surprisingly, the addition of Ni has been shown to increase the production of methane from mineral-poor peat samples, waste-water treatment facilities, and sewage sludge (for example, ref. 25). To put this into perspective, our data indicate that methanogenesis in the bulk oceans would have been Ni-stimulated throughout stage 1, and especially sensitive to plummeting Ni concentrations over the stage 1 to stage 2 transition, after which it remained in a state of strong Ni-limitation to the present day. Interestingly, methanogens do not appear to have abandoned their overall Ni dependency in the face of this famine (although some can produce nickel-free hydrogenases; see ref. 26 for review), perhaps because the biochemical re-tooling of so many energy-yielding metalloenzymes that are central to their metabolism was an obstacle too great to overcome. Cyanobacteria appear to have coped with changing metal availability over time by evolving metal-specific ligands (for example, ref. 8), but recent studies with methanogens have shown that they do not appear to produce Ni-specific ligands[27]. This may be due to (1) the relatively high solubility of Ni under both oxic and anoxic conditions[8], (2) the potentially high cost of ligand production[27], and (3) a lack of strong competition for Ni with other microorganisms. The fact that nickel concentrations in modern ocean surface waters are not as depleted as other bioactive metals[28] may indicate that the microbes that need it most can no longer access it due to the presence of oxygen.

Compounding this Ni famine would be waning fluxes of H_2 (their preferred reductant) with decreasing serpentinization of the sea floor (that is, $2Mg_{1.8}Fe_{0.2}SiO_4 + 2.933H_2O \rightarrow Mg_{2.7}Fe_{0.3}Si_2O_5(OH)_4 + 0.9Mg(OH)_2 + 0.033Fe_3O_4 + 0.033H_2$) accompanying the decrease in production of olivine-rich oceanic crust at the end of the 2.7-Gyr mantle plume event and the concomitant growth and stabilization of continental cratons[14,17]. It has been argued[29] that the shift from predominantly submarine volcanism to more subaerial volcanism further decreased abiotic H_2 fluxes because the latter yield more oxidized gases (H_2O, CO_2 and SO_2). In either case, a loss of H_2 would probably have contributed to a declining biogenic methane supply[30].

A drop in atmospheric methane around 2.4 Gyr ago has been invoked as the most parsimonious explanation for the onset of major Palaeoproterozoic glaciations, the ensuing demise of sulphur isotope mass-independent fractionation, and the progressive rise of atmospheric oxygen[1]. The authors of ref. 1 hypothesized that the biogenic methane flux would have waned owing to increasing competition between methanogens and sulphate-reducing microorganisms before 2.4 Gyr ago. Moreover, anaerobic oxidation of methane, a nickel-dependent process involving *Archaea* that appear to possess a variant of MCR that operates in reverse[31], would further have reduced methane escape with increasing sulphate concentrations at that time[32]. However, it is not until after the Great Oxidation Event that evidence in the rock record exists for pervasive oxidative weathering of terrestrial sulphides, a large oceanic sulphate pool, and the onset of widespread ocean euxinia (for example, refs 2, 3). We provide an alternative hypothesis, suggesting that the demise in large-scale methanogenesis occurred before, and was not necessarily related to, increasing environmental oxygenation. Our model provides a clear directionality in the evolution of the Earth's system, whereby a cooler mantle following the 2.7 Gyr event led to associated chemical changes in volcanism and trace element abundances in the oceans, triggering a decline in global methanogenesis, and ultimately facilitating the transition from anoxic to oxic atmospheric conditions some 2.4 Gyr ago. Thereafter, increased O_2 would have led to a larger oceanic sulphate pool, the end result being the marginalization of methanogens to anoxic and sulphate-poor niches, as is the case today.

METHODS SUMMARY

Ni and Fe contents representing 29 BIF were amassed from previously published bulk analyses ($n = 306$) as well as new analyses on both bulk ($n = 38$) and grain-by-grain (haematite and magnetite only; $n = 870$) scales. BIF samples were selected for low concentrations of Al (<1%) and incompatible elements (Ti, Zr, Th, Hf and Sc <20 p.p.m.) to avoid potential contamination from detrital components. Major elements were measured by electron microprobe (JOEL 8900), while trace element analyses were performed using a Perkin Elmer Elan6000 quadrupole ICP-MS (inductively coupled plasma mass spectrometer) operating in either solution mode for heated $HF+HNO_3$ whole-rock digests or using a New Wave Research UP213 laser ablation system (20–60 μm spot size) for grain-by-grain analysis of haematite and magnetite. Ni partitioning experiments were performed at ~23 °C in 0.5 M $NaNO_3$ to which 0.179 mM Fe (as ferrous ammonium sulphate hexahydrate) and various amounts of dissolved silica (0, 0.67 and 2.20 mM SiO_2, added as sodium silicate nonahydrate) were added. After an oxidation and equilibration period of 30 min, samples were filtered to 0.2 μm and analysed for Ni by quadrupole ICP-MS.

Full Methods and any associated references are available in the online version of the paper at www.nature.com/nature.

Received 27 August 2008; accepted 26 January 2009.

1. Zahnle, K. J., Claire, M. W. & Catling, D. C. The loss of mass-independent fractionation of sulfur due to a Paleoproterozoic collapse of atmospheric methane. *Geobiology* **4,** 271–283 (2006).
2. Papineau, D., Mojzsis, S. J. & Schmitt, A. K. Multiple sulfur isotopes from Paleoproterozoic Huronian interglacial sediments and the rise of atmospheric oxygen. *Earth Planet. Sci. Lett.* **255,** 188–212 (2007).
3. Scott, C. *et al.* Tracing the stepwise oxygenation of the Proterozoic ocean. *Nature* **452,** 456–459 (2008).
4. Bjerrum, C. J. & Canfield, D. E. Ocean productivity before about 1.9 Gyr limited by phosphorus adsorption onto iron oxides. *Nature* **417,** 159–162 (2002).
5. Konhauser, K. O., Lalonde, S. V., Amskold, L. & Holland, H. D. Was there really an Archean phosphate crisis? *Science* **315,** 1234 (2007).
6. Drever, J. I. *The Geochemistry of Natural Waters* 2nd edn (Prentice Hall, 1988).
7. Jaun, B. & Thauer, R. K. in *Metal Ions in Life Sciences* Vol. 2, *Nickel and its Surprising Impact in Nature* (eds Sigel, A., Sigel, H. & Sigel, R. K. O.) 323–356 (Wiley & Sons, 2007).
8. Saito, M. A., Sigman, D. M. & Morel, F. M. M. The bioinorganic chemistry of the ancient ocean: the co-evolution of cyanobacterial metal requirements and biogeochemical cycles at the Archean-Proterozoic boundary? *Inorg. Chim. Acta* **356,** 308–318 (2003).

9. Öztürk, M. Trends of trace metal (Mn, Fe, Co, Ni, Cu, Zn, Cd and Pb) distributions at the oxic-anoxic interface and in sulfidic water of the Drammensfjord. *Mar. Chem.* **48,** 329–342 (1995).
10. Hannington, M. D., Santaguida, F., Kjarsgaard, I. M. & Cathles, L. M. Regional-scale hydrothermal alteration in the Central Blake River Group, western Abitibi subprovince, Canada: implications for VMS prospectivity. *Mineralium Deposita* **38,** 393–422 (2003).
11. Keays, R. R. The role of komatiitic and picritic magmatism and S-saturation in the formation of ore deposits. *Lithos* **34,** 1–18 (1995).
12. Trendall, A. F. in *Precambrian Sedimentary Environments: A Modern Approach to Ancient Depositional Systems* (eds Altermann, W. & Corcoran, P. L.) 33–66 (Special Publication 33, International Association of Sedimentologists, 2002).
13. Berry, A. J., Danyushevsky, L. V., O'Neill, H. C., Newville, M. & Sutton, S. R. Oxidation state of iron in komatiite melt inclusions indicates hot Archaean mantle. *Nature* **455,** 960–963 (2008).
14. Barley, M. E., Krapež, B., Groves, D. I. & Kerrich, R. The Late Archaean bonanza: metallogenic and environmental consequences of the interaction between mantle plumes, lithospheric tectonics and global cyclicity. *Precambr. Res.* **91,** 65–90 (1998).
15. Kamber, B. S., Whitehouse, M. J., Bolhar, R. & Moorbath, S. Volcanic resurfacing and the early terrestrial crust: zircon U-Pb and REE constraints from the Isua Greenstone Belt, southern West Greenland. *Earth Planet. Sci. Lett.* **240,** 276–290 (2005).
16. Arndt, N. T. High Ni in Archean tholeiites. *Tectonophysics* **187,** 411–420 (1991).
17. Barley, M. E., Bekker, A. & Krapež, B. Late Archean to early Paleoproterozoic global tectonics, environmental change and the rise of atmospheric oxygen. *Earth Planet. Sci. Lett.* **238,** 156–171 (2005).
18. Nisbet, E. G. in *Komatiites* (eds Arndt, N.T. & Nisbet, E.G.) 501–520 (George Allen and Unwin, 1982).
19. Arndt, N. T., Barnes, S. J. & Lesher, C. M. *Komatiite* (Cambridge University Press, 2008).
20. da Silva, J. J. R. F. & Williams, R. J. P. *The Biological Chemistry of the Elements: The Inorganic Chemistry of Life* (Oxford University Press, 1991).
21. Jarrell, K. F., Colvin, J. R. & Sprott, G. D. Spontaneous protoplast formation in *Methanobacterium bryantii. J. Bacteriol.* **149,** 346–353 (1982).
22. Diekert, G., Weber, B. & Thauer, R. K. Nickel dependence of factor F_{430} content in *Methanobacterium thermoautotrophicum. Arch. Microbiol.* **127,** 273–278 (1980).
23. Schönheit, P., Moll, J. & Thauer, R. K. Nickel, cobalt, and molybdenum requirement for growth of *Methanobacterium thermoautotrophicum. Arch. Microbiol.* **123,** 105–107 (1979).
24. Kida, K. *et al.* Influence of Ni^{2+} and Co^{2+} on methanogenic activity and the amounts of coenzymes involved in methanogenesis. *J. Biosci. Bioeng.* **91,** 590–595 (2001).
25. Basiliko, N. & Yavitt, J. B. Influence of Ni, Co, Fe, and Na additions on methane production in *Sphagnum*-dominated Northern American peatland. *Biogeochemistry* **52,** 133–153 (2001).
26. Shima, S. & Thauer, R. K. A third type of hydrogenase catalysing H_2 activation. *Chem. Rec.* **7,** 37–46 (2007).
27. Hausrath, E. M., Liermann, L. J., House, C. H., Ferry, J. G. & Brantley, S. L. The effect of methanogen growth on mineral substrates: will Ni markers of methanogen-based communities be detectable in the rock record? *Geobiology* **5,** 49–61 (2007).
28. Saito, M. A., Moffett, J. W. & DiTullio, G. R. Cobalt and nickel in the Peru upwelling region: a major flux of labile cobalt utilized as a micronutrient. *Glob. Biogeochem. Cycles* **18,** GB4030 (2004).
29. Kump, L. R. & Barley, M. E. Increased subaerial volcanism and the rise of atmospheric oxygen 2.5 billion years ago. *Nature* **448,** 1033–1036 (2007).
30. Kharecha, P., Kasting, J. & Siefert, J. A coupled atmosphere-ecosystem model of the early Archean Earth. *Geobiology* **3,** 53–76 (2005).
31. Krüger, M. *et al.* A conspicuous nickel protein in microbial mats that oxidize methane anaerobically. *Nature* **426,** 878–881 (2003).
32. Catling, D. C., Claire, M. W. & Zahnle, K. J. Anaerobic methanotrophy and the rise of atmospheric oxygen. *Phil. Trans. R. Soc. A* **365,** 1867–1888 (2007).

Supplementary Information is linked to the online version of the paper at www.nature.com/nature.

Acknowledgements We thank M. Labbe for sample preparation, G. Chen and A. Simonetti for assistance with LA-ICP-MS analyses in the Radiogenic Isotope Facility at the University of Alberta, and S. Matveev for assistance with electron microprobe analyses. Field assistance by W. Mueller is acknowledged for Hunter Mine Group samples. Samples from the Loch Maree Group were provided by A. Wright. Funding was provided by the Natural Science and Engineering Research Council of Canada (NSERC) to K.O.K., the Canada Research Chairs Program to B.S.K., the Australian Research Council (ARC) to M.E.B., and NASA Exobiology and Evolutionary Biology Program individually to D.P. and K.Z. This manuscript was improved by discussions with R. Buick, J. Kasting and M. Lesher, and reviews by R. Frei and M. Saito.

Author Contributions BIF samples were provided by K.O.K., E.P., B.S.K. and D.P. E.P. performed LA-ICP-MS and electron microprobe analysis and S.V.L. conducted sorption experiments. K.O.K., S.V.L., E.P. and B.S.K. produced the manuscript with significant contributions from all co-authors. Specifically, insights into komatiites were provided by E.G.N., N.T.A. and M.E.B.; early Earth tectonics by M.E.B. and B.S.K.; and GOE and methanogens by D.P. and K.Z.

Author Information Reprints and permissions information is available at www.nature.com/reprints. Correspondence and requests for materials should be addressed to K.O.K. (kurtk@ualberta.ca).

METHODS

Sample selection. High abundances of Ni have been recorded in several Archaean clastic sedimentary rocks, and have generally been explained by the presence of an ultramafic dominated crustal source (for example, refs 33, 34). Average compositions of post-Archaean clastic sedimentary rocks define a progressive decrease in Ni concentrations through time, which is clearly related to a compositional change in the upper continental crust[35]. Even though this decrease parallels the trend recorded in BIF, both in time and Ni/Fe concentration, reliable authigenic trace metal contents can be compromised by contamination with siliciclastic or volcanic inputs. Therefore, our interpretation of the Ni signal in BIF as a genuine reflection of palaeoseawater required a pre-selection of BIF samples with minimal detrital influence based on chemical composition (as below).

One method commonly used to differentiate detritally sourced components versus authigenic precipitation is through measurement of incompatible, immobile elements such as Al, Ti, Zr, Th, Hf, and Sc (ref. 36). Thus, data presented in Supplementary Tables 1 and 2 were selected according to the following criteria: (1) $<$1 wt% Al, (2) low concentrations ($<$20 p.p.m.) of Ti, Zr, Th, Hf and Sc, and (3) on the basis of lack of co-variations of Zr versus Y/Ho; Y/Ho versus Ce/Ce*; and Th versus La/La* (for example, refs 37, 38). Furthermore, samples noted or reported to contain sulphides were avoided, to minimize the influence of post-depositional hydrothermal activity on our data set. Through the use of these filters, we are confident that our BIF samples reflect precipitation from sea water.

Ni analyses in BIF. Data are presented in Supplementary Tables 1 and 2. Selected BIF samples for geochemical analyses include both drill core and hand samples from fresh exposures. Oxidized surfaces, veins and samples with pyrite were avoided to minimize the effects of weathering and post-depositional overprinting.

For bulk trace element analyses, samples were cut into slabs and broken into small chips ($<$5 mm) without metal contact. Subsequently, between 20 and 150 g of the material was powdered in an automated agate mill. Crushed rock powders ($<$100 mesh) were completely dissolved with heated HF+HNO_3 and analysed using a Perkin Elmer Elan6000 Quad-ICP-MS (quadrupole inductively coupled plasma mass spectrometer). Accuracy and precision of the analytical protocol were verified with the use of well-established international whole rock standards (for example, BE-N Basalt, CRPG Nancy; see http://research.eas.ualberta.ca/rif/quad_icp_ms.html).

In situ trace element analyses were performed on haematite and magnetite grains using a quadrupole ICP-MS coupled to a laser ablation system (spot size 20–60 μm in diameter). Haematite was chosen as proxy for the original precipitates as it probably formed from dehydration of hydrous ferric oxide (HFO) precursors, and it provides a means of direct comparison between BIF samples of significantly different bulk composition. As magnetite is generally regarded as a secondary iron oxide phase formed by partial reduction of HFO or haematite, we used it to assess post-depositional Ni/Fe disturbances. In this regard, no significant differences between the two iron oxide minerals were observed.

Optimization of ICP-MS instrument parameters (RF power 1,200 W, peak hopping acquisition, 50 ms dwell time) were achieved by ablating either the NIST SRM 610 ($\sim$500 p.p.m.) or NIST SRM 612 ($\sim$50 p.p.m.) international glass standards. For quantitative trace element determinations, the NIST 610 (for 20 μm spot size) and 612 (for 60 μm spot size) standards and BIF samples were ablated using identical conditions with spot sizes of either 20 μm or 60 μm, 5 Hz repetition rate and energy density of $\sim$13 J cm^{-2}. Quantitative results were obtained via the calibration of relative element sensitivities against the NIST 610 and 612 standards, while Fe values from electron microprobe analyses (JOEL 8900, University of Alberta) were used as internal standards. Data reduction and concentration determinations were obtained using the GLITTER (XP version, New Wave Research) laser ablation software. Repeated analysis ($n = 10$) of the NIST 612 using a 60 μm spot size yielded relative standard deviations of between 5 and 15% (2σ level) and detection limits between 0.2 (for example, Cu) and 3 p.p.m. (for example, Cr) for most elements (except for P $\sim$13 p.p.m., Fe $\sim$20 p.p.m. and Ca $\sim$165 p.p.m.). All new BIF measurements reported here were performed in the Radiogenic Isotope Facility at the Department of Earth and Atmospheric Sciences, University of Alberta.

Statistical treatment of the data are outlined in Supplementary Table 2, and graphically presented in Supplementary Figs 1, 2 and 3. Ni values were normalized on a molar ratio basis to total Fe for all bulk and laser-ablation analyses because (1) the similar Ni/Fe values observed between individual haematite and magnetite grains indicates that we cannot exclude Fe(II)-containing phases as significant sources of Ni, and (2) many of the published bulk analyses do not discriminate between Fe(II) and Fe(III).

Ni partitioning experiments. Concentrated ferrous iron stock solutions (0.1074 M) were freshly prepared at pH $\sim$3 from ferrous ammonium sulphate hexahydrate and diluted to 0.179 mM in pH 7 receiving solutions consisting of 0.5 M $NaNO_3$ and various amounts of silica (0, 0.67 mM and 2.20 mM, added as sodium metasilicate nonahydrate) and dissolved nickel (0–4,000 nM). These dissolved silica concentrations were chosen to span conditions ranging from as high as amorphous silica saturation (2.20 mM), to cristobalite saturation (0.67 mM), and to modern oceans largely stripped of dissolved silica, in order to explore the effects of dissolved silica on Ni partitioning to iron oxides through time. The oceans were at least saturated with cristobalite, and probably amorphous silica, before 1.8 Gyr ago[39], only to achieve modern values in the Phanerozoic ($<$0.10 mM)[40] with the advent of silica-secreting eukaryotes.

Dissolved nickel was sourced from a 1,000 p.p.m. Ni commercial ICP-MS standard (in 2% HNO_3, SPEX CertiPrep). All experiments were performed at $\sim$23 °C in acid-washed glassware with continuous mixing. The pH values of all experiments were monitored continuously and maintained at pH 7 by the addition of dilute HCl or NaOH. After an Fe(II) oxidation and equilibration period of 30 min, samples were filtered through 0.2 μm nylon in-line syringe filters, acidified with trace-metal grade HNO_3, and analysed within one week for Ni, as well as for Fe (to confirm complete oxidation and precipitation), by ICP-MS (Perkin Elmer Elan6000) at the University of Alberta.

33. McLennan, S. M., Taylor, S. R. & Eriksson, K. A. Geochemistry of Archean shales from Pilbara Supergroup, Western Australia. *Geochim. Cosmochim. Acta* **47,** 1211–1222 (1983).
34. Taylor, S. R. & McLennan, S. M. *The Continental Crust: Its Composition and Evolution* (Blackwell, 1985).
35. Condie, K. C. Chemical composition and evolution of the upper continental crust: contrasting results from surface samples and shales. *J. Chem. Geol.* **104,** 1–37 (1993).
36. Chester, R. *Marine Geochemistry* (Blackwell, 2000).
37. McLennan, S. M. in *Geochemistry and Mineralogy of Rare Earth Elements* (eds Lipin, B. R. & McKay, G. A.) 169–200 (Mineral Society of America, 1989).
38. Kamber, B. S. & Webb, G. E. The geochemistry of late Archaean microbial carbonate: implications for ocean chemistry and continental erosion history. *Geochim. Cosmochim. Acta* **65,** 2509–2525 (2001).
39. Maliva, R. G., Knoll, A. H. & Simonson, B. M. Secular change in the Precambrian silica cycle: insights from chert petrology. *Geol. Soc. Am. Bull.* **117,** 835–845 (2005).
40. Tréguer, P. *et al.* The silica balance in the world ocean: a reestimate. *Science* **268,** 375–379 (1995).